Examination of Large-Scale Dust Explosion Reactivity by Decoupling Dust Injection and Turbulence Generation

C. Regis L. Bauwens, Lorenz R. Boeck, Sergey B. Dorofeev
FM Global, Research Division
Norwood, MA, USA

1 Introduction

While dust explosion hazards can be present anywhere combustible dusts are handled, there are several highly effective measures that can mitigate these events. An understanding of the underlying reactivity of the dust present is required, however, to properly assess the explosion hazard and determine the most appropriate explosion protection strategy. Numerous studies have attempted to define fundamental dust reactivity parameters, such as dust laminar burning velocities [1, 2, 3], but as of yet there is no universally consistent method to quantify these values or translate them into applied models for industrial-scale explosions. Instead, empirical dust reactivity measures, predominantly the dust's deflagration index K_{St}, which was originally defined to provide a relative ranking of dust reactivity, are used to quantify dust reactivity for explosion protection purposes [4]. Studies have suggested, however, that K_{St} values obtained in small-scale standardized tests may not be fully representative of large-scale behavior [5], where large-scale tests have demonstrated that dusts with significantly lower values of K_{St} can sometimes produce more severe consequences under nominally identical experimental conditions.

Currently, K_{St} is determined by standardized tests in a 20-L or 1-m^3 spherical apparatus. These test setups are calibrated with strictly defined ignition delay times, typically measured from the start of dust injection, to provide a standard method of testing under what is believed to be nominally identical conditions. In these tests, the value of K_{St} is obtained by examining the pressure transient within the vessel during a dust explosion and normalizing the maximum rate of pressure rise by the vessel volume, V as follows:

$$K_{St} = \left(\frac{dP}{dt}\right)_{\max} V^{1/3}.$$

It should be noted that in these standard tests, as well as in the vast majority of dust explosion research studies, the process of dust injection and turbulence generation is highly coupled, where each injector performs both tasks simultaneously. This is important, as the level of initial turbulence drives the measured reactivity [6, 7], where shorter ignition delays produce higher rates of pressure rise, while longer ignition delays allow more time for turbulence decay and result in lower rates of pressure rise. Furthermore, in large-scale testing with vessels that are not standardized, an effective deflagration index, K_{eff} is typically used and tuned by varying the ignition delay to achieve a desired level of reactivity.

Correspondence to: carl.bauwens@fmglobal.com

In this study, a new experimental test setup is developed in a 2.5-m^3 vessel with the goal of decoupling the dust injection and turbulence generation processes. Using this setup, six different dusts are examined over a range of turbulent conditions, by varying the ignition delay, to develop a better understanding of the variation of dust reactivity with dust properties and turbulence. This work also aims to examine whether K_{St} and K_{eff} are appropriate reactivity parameters that capture the behavior of the different dusts through comparison with measurements obtained from standard 20-L sphere testing. Finally, this study will use a previously developed dust combustion model to gain additional insight into how the experimental results can be interpreted and see how well the behavior of the dusts can be characterized using a different set of reactivity parameters.

2 Experimental Setup

The experiments were performed in a 2.5-m^3 vessel with a height to diameter ratio of 1.45, as shown in Fig. 1 (left). Dust and air were injected into the vessel prior to ignition using two counterflow injection systems, which were each comprised of two air cannons, a sealed dust hopper, an explosion isolation valve, and an internal dispersion nozzle. For each injector, two Martin® Hurricane 35-L air cannons, Fig. 1 (right), pressurized to 8.3 barg, were used to inject dust and generate turbulence. These injectors were timed to fire in series with a prescribed delay, such that the first injector fully dispersed the dust into the vessel while the second injector generated initial turbulence. In all of the tests, the mixture was ignited at the center of the vessel by two 5-kJ Sobbe EBBOS ChZ pyrotechnic ignitors. Within the vessel, pressure was measured at three elevations, however, all internal pressure measurements were effectively identical, so only the transducer at the center height was used in the following analysis.

Figure 1: An image of the 2.5-m^3 test vessel setup showing both dust injectors (left) as well as an image of the dual air cannon configuration (right).

For this study, six different dusts were examined, as summarized in Table 1. These dusts were selected in order to cover a wide range of dust properties, including bulk density, ρ_{bulk}, melting point, T_{melt}, and median particle size, $D50$. The dust loading, m_{d}/V, which was used for each dust, is also show in Table 1.

The following procedure was used to perform each individual test. First, the dust hoppers were loaded with a prescribed mass of dust to achieve the target dust loading. Next, the vessel was evacuated to a specified pressure, approximately 0.5 bar, that was varied to compensate for differences in the initial gas temperature between tests in order to obtain a final pressure of 1.00 ± 0.02 bar after both air cannons had been fired. Finally, a high-precision timing sequence fired the dust injection air cannon, followed by the turbulence generation air cannon, followed by the ignition system using a series of time delays described below.

Table 1: Properties of the dusts and the dust loadings examined.

Dust	K_{St} (bar m/s)	ρ_{bulk}	T_{melt} (°C)	$D50$ (µm)	m_d/V (kg/m^3)
Cornstarch	160	610	-	14	0.75
Cellulose fiber	75	140	260	78	0.50
Powdered sugar	57	657	186	26	0.75
Lycopodium	141	320	-	30	0.75
Durez 32580	198	433	94	21	0.50
Irganox MD 1024	325	350	229	36	0.50

Three primary ignition delays were adopted, defined here as the time between the firing of the second air cannon and ignition, by determining the delays that produced K_{eff} values of $K_{eff} \approx 300$ bar m/s, $K_{eff} \approx 200$ bar m/s, $K_{eff} \approx K_{St} \approx 160$ bar m/s for cornstarch with a dust loading of $m_d/V = 0.75$ kg/m^3. The firing arrangement of the two air cannons associated with the same injector was timed to create a 1.0-second delay between the firing of the first air cannon, to inject the dust, and the firing of the second air cannon, to generate turbulence. To ensure this delay was sufficiently long to fully inject the dust and not impact the turbulence generation process, additional tests were also performed with a time delay of 0.5 s between dust and air injection, and these tests were found to be indistinguishable from the tests performed with a 1.0-s delay. The need for, and performance of, this dust injection system is illustrated in Fig. 2 for a series of tests performed with a dust loading $m_d/V = 0.5$ kg/m^3. The dust injection profiles, Fig. 2 (left), demonstrate that, even though equivalent masses of dust are being injected, the properties of the dust themselves significantly affect the injection process. This results in an approximately 75 ms variability in the time taken for the dust injection air cannon to fully inject the different dusts, compared to the air injection pressure transients, Fig. 2 (right), that are virtually indistinguishable from one another. The variability in dust injection times is significant, as the ignition delays used in this study are only on the order of 180 – 410 ms and without the second air cannon, the 75 ms difference in injection time would have a significant effect on the level initial turbulence present at the time of ignition.

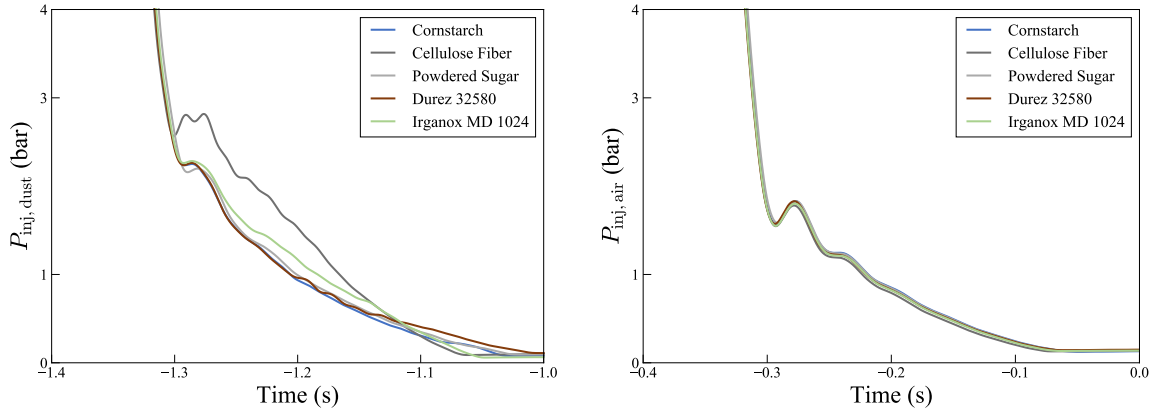

Figure 2: Pressure decay transient of the dust injection air cannon (left) and subsequent pressure decay transient of the air injection cannon (right).

3 Model Description

To further analyze the experimental results and examine the role of the underlying dust properties on overall dust reactivity, a previously developed dust combustion model [8] was used. The simple two-

parameter model characterizes dust combustion by a turbulent flame propagation velocity $S_{T,0}$, which defines the propagation rate of the leading edge of the flame, and a characteristic combustion time, which is characterized by a dimensionless parameter χ. While the turbulent propagation velocity was found to generally characterize the initial rate of pressure rise and scales with the magnitude of the maximum rate of pressure rise, the parameter χ governed the overall shape of the pressure profile. This can be easily seen when plotting the rate of pressure rise for different values of χ in dimensionless terms, as shown in Fig. 3, where P_m is the maximum explosion pressure and P_0 is the initial pressure at the time of ignition. To obtain these parameters from an individual test, a fitting routine was developed to automatically fit the model results against the experimentally obtained pressure transient.

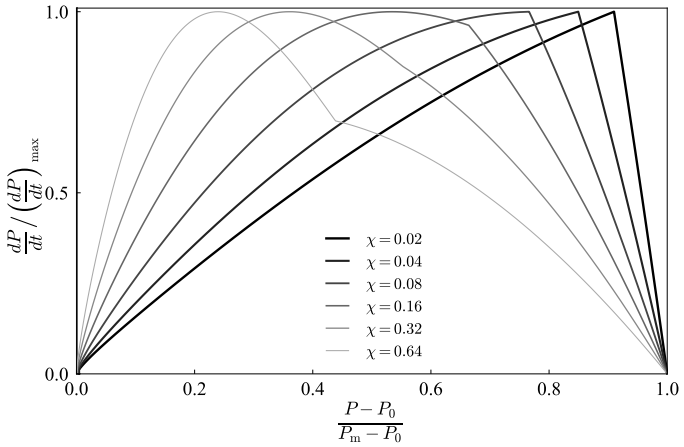

Figure 3: Generalized model results as a function of normalized pressure for a range of the dimensionless parameter χ.[8]

4 Results and Discussion

For the results presented below, 35 large-scale experiments were performed for the six different dusts across a range of ignition delays. The variation in measured K_{eff} as a function of ignition delay is plotted in Fig. 4 (left). Across all of the dusts, it can be seen that there is a roughly linear increase in K_{eff} with decreased ignition delay. Also, these results clearly show that the values of K_{eff} obtained for the different dusts do not follow the same relative ranking provided by the values of K_{St} listed in Table 1. For example, the most reactive dust, Iraganox MD 1024, with a K_{St} twice that of cornstarch, produces significantly lower maximum rates of pressure rise in the large-scale tests. Furthermore, when comparing the rate of pressure rise as a function of dimensionless pressure, Fig. 4 (right), cornstarch demonstrates a higher rate of pressure rise across the entire explosion event. This figure also demonstrates how the different dusts exhibit a maximum rate of pressure rise at different dimensionless pressures.

When compared with the dust combustion model results, it was found that the parameters $S_{T,0}$ and χ captured the overall rate of pressure rise transient well across all of the dusts studied, as shown in Fig. 4 (right). When examining the fitted values for the turbulent propagation velocity, Fig. 5 (left), it can be seen that $S_{T,0}$ varied linearly with ignition delay, much like K_{eff}. The relative ranking of these values, however, is now roughly in agreement with that suggested by the K_{St} values obtained from 20-L sphere testing.

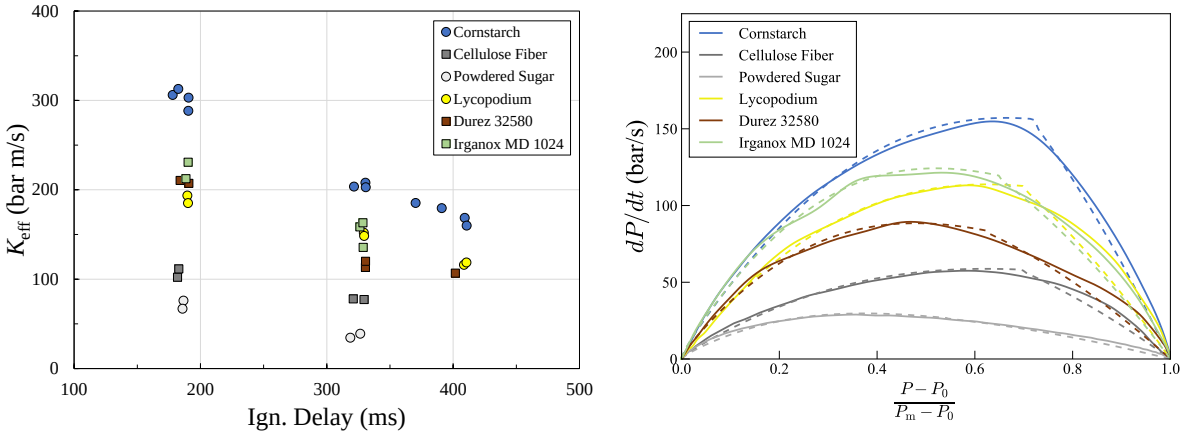

Figure: 4. Measured K_{eff} as a function of ignition delay for all of the dust examined (left) and a comparison of experimental rate of pressure rise as a function of dimensionless pressure for representative experiments performed with an ignition delay of 330 ms including model best fits (dashed lines).

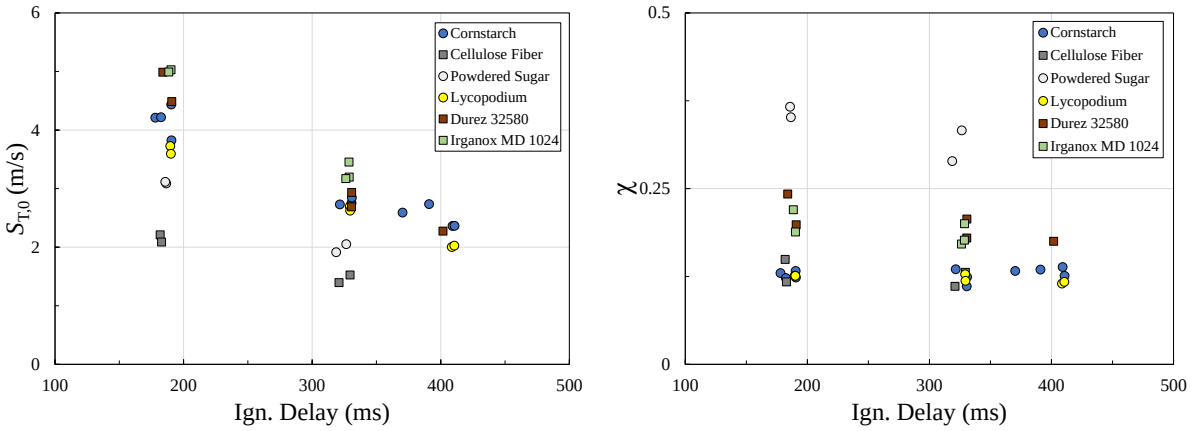

Figure 5: Modeled fits for the values of $S_{T,0}$ (left) and χ (right) obtained from the experimental results.

It is interesting to note, however, that the model fits for the different fuels yielded significantly different values of χ, as shown in Fig. 5 (right), and these values appear largely independent of ignition delay, at least across the range of ignition delays examined. For the different dusts, ranges of χ can be seen with cornstarch ($\chi = 0.13 \pm 0.02$), cellulose fiber ($\chi = 0.13 \pm 0.02$), and lycopodium ($\chi = 0.12 \pm 0.01$) all being roughly equivalent. Next, it can be seen that Durez 32580 ($\chi = 0.20 \pm 0.04$) and Irganox MD 1024 ($\chi = 0.19 \pm 0.03$) occupy the middle range and are also similar to one another. Finally, the powdered sugar results yielded the highest values of χ ($\chi = 0.33 \pm 0.04$). The independence of χ with ignition delay and its strong variation between different dusts implies that the value of χ depends primarily on the material properties of the dust. These results will be directly used in future work examining how χ varies with different dust properties to develop improved models for dust explosion protection.

5 Summary and Conclusions

In this study, a new dust explosion test setup was developed that effectively decouples the dust injection process from turbulence generation, allowing for better comparisons between dusts under effectively equivalent conditions. Using this setup, six different dusts were tested over a range of ignition delays. The results clearly demonstrate that the relative ranking provided by K_{St} measurements in 20-L sphere testing does not necessarily align with the actual reactivity found in large-scale tests, indicating significant limitations with the standard K_{St} reactivity methodology.

When compared with a previously developed dust combustion model, it was found that the model could characterize the overall dust explosion process using only two parameters, $S_{\mathrm{T},0}$ and χ, for all examined dusts. These two parameters were found to decouple the combustion behavior into a parameter that primarily varies with initial turbulence, and a parameter that varies with the inherent properties of the dust. Using these results, future models can be developed to better understand what fundamental dust properties are responsible for these differences and develop better mitigation strategies for the hazards presented by different combustible dusts.

References

[1] Goroshin, S., I. Fomenko, J. H. S. Lee. (1996) "Burning velocities in fuel-rich aluminum dust clouds." In Symposium (International) on Combustion, vol. 26(2): 1961-1967.

[2] Van Wingerden, K., Stavseng, L., Bergen, N. (1996). Measurements of the laminar burning velocities in dust-air mixtures. VDI-Berichte, *1272:* 553-564.

[3] Julien, P., Vickery, J., Goroshin, S., Frost, D. L., Bergthorson, J. M. (2015). Freely-propagating flames in aluminum dust clouds. Combustion and Flame, 162(11): 4241-4253.

[4] Eckhoff, R.K. (2003). Dust explosions in the process industries. Third edition. Gulf Professional Publishing, Amsterdam.

[5] Eckhoff, R. K. (2015). Scaling of dust explosion violence from laboratory scale to full industrial scale–A challenging case history from the past. Journal of Loss Prevention in the Process Industries, 36: 271-280.

[6] Amyotte, P. R., Chippett, S., Pegg, M. J. (1988). Effects of turbulence on dust explosions. Progress in Energy and Combustion Science, 14(4): 293-310.

[7] Tamanini, F, (1998). The role of turbulence in dust explosions. Journal of Loss Prevention in the Process Industries, 11(1): 1-10.

[8] Bauwens, C.R.L, Boeck, L.R., Dorofeev, S.B., Characterizing the reactivity of large-scale dust explosions, 28th International Colloquium on the Dynamics of Explosions and Reactive Systems. Naples, Italy, June 19-24, 2022.